JOURNAL OF VIROLOGY, Dec. 2007, p. 13578–13586 Vol. 81, No. 24
0022-538X/07/$08.00+0 doi:10.1128/JVI.01663-07

X Box Binding Protein XBP-1s Transactivates the Kaposi's Sarcoma-Associated Herpesvirus (KSHV) ORF50 Promoter, Linking Plasma Cell Differentiation to KSHV Reactivation from Latency▽

Sam J. Wilson,[1] Edward H. Tsao,[1] Benjamin L. J. Webb,[1] Hongtao Ye,[2] Lucy Dalton-Griffin,[1] Christoforos Tsantoulas,[1] Catherine V. Gale,[1] Ming-Qing Du,[2] Adrian Whitehouse,[3] and Paul Kellam[1]*

Department of Infection, UCL, Cleveland Street, London W1T 4JF,[1] Department of Pathology, University of Cambridge, Tennis Court Road, Cambridge CB2 1QP,[2] and Institute of Molecular and Cellular Biology, Faculty of Biological Sciences, University of Leeds, Leeds LS2 9JT,[3] United Kingdom

Received 31 July 2007/Accepted 28 September 2007

Reactivation of lytic replication from viral latency is a defining property of all herpesviruses. Despite this, the authentic physiological cues for the latent-lytic switch are unclear. Such cues should ensure that viral lytic replication occurs under physiological conditions, predominantly in sites which facilitate transmission to permissive uninfected cells and new susceptible hosts. Kaposi's sarcoma-associated herpesvirus (KSHV) is associated with the B-cell neoplasm primary effusion lymphoma (PEL), in which the virus remains latent. We have previously shown that PEL cells have the gene expression profile and immunophenotype of cycling preplasma cells (plasmablasts). Here, we show that the highly active spliced isoform of plasma cell transcription factor X box binding protein 1 (XBP-1s) is a lytic switch for KSHV. XBP-1s is normally absent in PEL, but the induction of endoplasmic reticulum stress leads to XBP-1s generation, plasma cell-like differentiation, and lytic reactivation of KSHV. XBP-1s binds to and activates the KSHV immediate-early gene ORF50 and synergizes with the ORF50 gene product RTA to induce a full lytic cycle. These data suggest that KSHV remains latent until B-cell terminal differentiation into plasma cells, the transcriptional environment of which provides the physiological "lytic switch" through XBP-1s. This links B-cell terminal differentiation to KSHV lytic reactivation.

Kaposi's sarcoma-associated herpesvirus (KSHV), or human herpesvirus 8, is the etiological agent of Kaposi's sarcoma (8) and is also associated with the B-cell neoplasm primary effusion lymphoma (PEL) (6) and a subset of multicentric Castleman's disease (10). Like all herpesviruses, KSHV has the ability to latently infect cells, thereby persisting without producing progeny virions. Latent KSHV retains the capacity to reactivate in response to the appropriate physiological cues, and the regulation of this reactivation is important for understanding viral transmission and disease pathogenesis. Various nonphysiological treatments can cause reactivation of latent KSHV in vitro, but the cellular events resulting in reactivation in vivo remain unclear. These events must also explain the production of KSHV in oral and genital secretions, which are the most likely routes of horizontal transmission (31).

All PEL cells harbor latent KSHV and are phenotypically similar to B cells arrested immediately prior to terminal differentiation into antibody-secreting plasma cells (20, 22). Terminal differentiation into antibody secreting plasma cells is an important component of the immune response. To attain a secretor phenotype, B cells must expand their secretory apparatus during differentiation (35, 38). This is achieved by inducing part of the unfolded protein response (UPR), a well-characterized stress response to an increased protein-folding burden within the endoplasmic reticulum (ER) (34). Utilizing a "physiological UPR," B cells expand their secretory apparatus during differentiation (18).

The UPR is a tightly regulated response to ER stress that is detected and initiated by binding of the protein Grp78/BiP to protein motifs indicative of misfolded proteins in the ER (14). This removes BiP from its "normal" cellular binding partners, including inositol requiring enzyme 1 (IRE1) (2). IRE1 subsequently homodimerizes and following autophosphorylation forms a complex competent to catalyze the endonucleolytic processing of X box binding protein 1 (XBP-1) mRNA (36). Under conditions free from ER stress, XBP-1 mRNA encodes a 33-kDa protein from unspliced XBP-1 mRNA (XBP-1u). Under ER stress, IRE1 catalyzes the removal of a 26-nucleotide intron from XBP-1u mRNA, resulting in a frame shift within the coding region leading to the translation of a more stable, 54-kDa transcription factor, XBP-1s (5). XBP-1s is a basic leucine zipper (bZIP) transcription factor containing a potent C-terminal transcriptional activation domain and is involved in many of the transcriptional changes required to expand a cell's secretory capacity (35). XBP-1s expression is required for the expansion of the secretory apparatus associated with the terminal differentiation of most B-cell subsets (33).

In the majority of instances, PEL resembles a transformed postgerminal-center B cell (13, 26). PEL cells express CD138

* Corresponding author. Mailing address: Department of Infection, UCL, 46 Cleveland Street, London W1T 4JF, United Kingdom. Phone: 44 20 7679 9559. Fax: 44 20 7679 9555. E-mail: p.kellam@ucl.ac.uk.

▽ Published ahead of print on 10 October 2007.

(syndecan-1) (15) and B-lymphocyte-induced maturation protein 1 (BLIMP-1), which are associated with late stages of B-cell differentiation. Transcriptional profiling of PEL cells indicates that PEL cells are representative of mature preterminally differentiated plasmablasts (20, 22). These plasmablasts express but have an incomplete upregulation of genes associated with the UPR. Whereas most cases of PEL have functional immunoglobulin (Ig) gene rearrangements and express Ig mRNA, most do not express Ig protein (26, 27). Since PEL cells do not secrete Ig but are almost fully differentiated, we investigated the status of XBP-1 expression in PEL and determined if B-cell terminal differentiation through XBP-1s is a cue for KSHV lytic reactivation.

Here, we demonstrate that XBP-1 mRNA is unspliced in PEL cell lines but that they retain the ability to process XBP-1 mRNA in response to ER stress. XBP-1s binds the KSHV ORF50 promoter and potently upregulates KSHV ORF50 expression, thereby inducing KSHV lytic replication. This supports similar recent data regarding murine XBP-1s (43). XBP-1s therefore links plasma cell differentiation to KSHV lytic replication.

MATERIALS AND METHODS

Cell culture. All cell lines were grown in RPMI 1640 medium (Invitrogen) with 10% fetal calf serum (BioSera) and 100 units/ml penicillin-streptomycin (Invitrogen) in 5% CO_2 at 37°C, except for HEK 293T BAC36-6 cells, HEK 293T r219-9, and HEK 293T cells, which were cultured in Dulbecco's modified Eagle's medium (Invitrogen) with 10% fetal calf serum and 100 units/ml penicillin-streptomycin. To induce a UPR, 5×10^7 JSC-1 and BC-3 PEL cell lines were cultured in medium containing 2 mM dithiothreitol (DTT).

RNA extraction and reverse transcriptase-PCR (RT-PCR). Total RNA was purified from 5×10^6 cells with TRIzol (Invitrogen), treated with DNase (Promega), and repurified by phenol extraction followed by ethanol precipitation. Oligonucleotide dT (Promega)-primed cDNA was used for PCR amplification across the XBP-1 atypical splice junction, using the primers XBP-1 forward (5′-CCT TGT AGT TGA GAA CCA GG-3′) and XBP-1 reverse (5′-CAG AAT GCC CAA CAG GAT ATC-3′). The PCR cycle consisting of 95°C for 30 seconds, 55°C for 30 seconds, and 72°C for 1 min was repeated 40 times. Twenty units of PstI (Promega) was added where necessary to the 50-μl PCR mixtures and incubated overnight at 37°C prior to electrophoresis.

Immunofluorescence and flow cytometry. PEL cells (1×10^6) were fixed in 4% formaldehyde (TAAB) prior to permeabilization with phosphate-buffered saline containing 0.1% Triton X-100 (Sigma). PEL cells were then incubated in the presence of a monoclonal IgG against RTA (26) diluted 1:2,000. Cells were then washed four times and incubated with an allophycocyanin-conjugated goat anti-mouse IgG (Biolegend) before being washed again four times prior to analysis by flow cytometry (Becton Dickinson LSR). Granularity was assessed using live PEL cells by analyzing 100,000 cells washed twice in phosphate-buffered saline. Histograms and density plots were generated using WinMDI (Scripps).

Immunocytochemistry. Cells were mixed with appropriate volumes of plasma and bovine thrombin (Diagnostic Reagents Ltd., Oxon, United Kingdom) to form a cell clot and then fixed in formalin and paraffin embedded with standard procedures. Four-micrometer sections were immunostained with anti-KbZIP rabbit antibody (32) (1:400 dilution) for 1 h, followed by incubation with biotinylated swine anti-rabbit antibody (DAKO, Denmark) and peroxidase-conjugated ExtroAvidin. The staining was visualized with DAB (3,3-diaminobenzidine tetrahydrochloride) and counterstained with hematoxylin.

Luciferase promoter assays. 293T cells were transfected using 2 μg of the appropriate DNAs. After 48 h, cells were harvested in 200 μl of passive lysis buffer (Promega). Quantitation of relative light units was determined using the dual luciferase Stop & Glo reagent in accordance with the manufacturer's instructions (Promega) and a Berthold luminometer (EG & G Berthold) with a dual injector system. All assays were performed in triplicate.

Lentiviral vector construction. Lentiviral vector-genomes pXBPsIG and pXBPuIG were generated through PCR amplification of XBP-1 from SK-MM-2 cDNA by using *Taq* polymerase (Promega) in accordance with the manufacturer's instructions and the oligonucleotide primers XBP-1F (5′-GGA AGA TCT TCG GAT CCC GCA ATT GGT CTG GAG CTA TGG TGG TGG CAG CCG-3′) and XBP-1RC (5′-ATA GTT TAG CGG CCC AAC TCG AGT CAG TGG TGG TGG TGA TGG TGG ACA CTA ATC AGC TGG GGA AAG AGT TC). The XBP-1RC primer encodes a six-His tag (only XBP-1s is tagged). PCR products were cloned using pGEM-T-Easy, sequenced, and subcloned into the lentiviral vector-genome pCSBX/pIG by using BamHI and XhoI (pXBPuIG) or subcloned into pEMW by using BamHI and XhoI prior to insertion into pIG, using BamHI and NotI (pXBPsIG). Plasmids pIG, pXBPsIG, and pXBPuIG all encode emerald green fluorescent protein (EmGFP) downstream of an encephalomyocarditis virus internal ribosome entry site.

The lentiviral vector G-P, which expresses short hairpin RNA (shRNA)-GFP, was described previously (9), and lentiviral vector X-P was generated using oligonucleotide 5′-CGA AAA AGA CTG CCA GAG ATC GAA AGA AGG CGA ACC TTC TCT CAA TCT CCG GCA GTC GGT GTT TCG TCC TTT CCA CAA GAT-3′ and T7 oligonucleotide 5′-TAA TAC GAC TCA CTA TAG GG-3′ to PCR amplify an shRNA expression cassette, using pGEM-U6L as a template (9). This amplicon was cloned using pGEM-T-Easy (Promega) and inserted into pCSPW as described previously (9). The shRNA sequences are therefore shRNA-GFP (5′-GUU CAU CUG CAC CAC CGG CAA GCU UCG GCU UGC CGG UGG UGC AGA UGA ACU U-3′) and shRNA-XBP)5′-GAC UGC CGG AGA UUG AGA GAA GGU UGC CCU UCU UUC GAU CUC UGG CAG UCU U-3′). Lentiviral vectors were produced as described previously (3). Briefly, HEK 293T cells were transfected with 1 μg of p8.91, 1 μg of pMDG, and 1.5 μg of lentiviral vector genome, using FuGENE-6 (Roche). Filtered supernatants were collected at 48 and 72 h posttransfection and titrated on HEK 293T cells.

p50Redi reporter assays. Plasmid p50Redi was constructed by amplifying a 4,099-bp region of the ORF50 promoter, first exon, intron, and the first 7 codons of the second exon, using the PCR primers ORF50Redi forward (5′-CGC TCC ATT AAT TGG AAG CAT TCT CTC TTC ATC GTG TGT GC-3′) and ORF50Redi reverse (5′-AAG CTT GCT AGC GCG GAC CGC CGA AGC TTC TTA CCC TAA GGA G-3′). The amplicon was digested with AseI and NheI and ligated with AseI- and NheI-digested pCMV-DsRed-express (Clontech). HEK 293T cells were transfected with 1 μg of p50Redi or deletion thereof and 2.8 μg of pXBPsIG or the molar equivalent of other expression plasmids. A total mass of 3.8 μg for all transfections was achieved by adding pBluescript II KS+. At 48 h posttransfection, cells were harvested and EmGFP and DsRed-express expression was quantified using flow cytometry. In experiments delivering two transcription factors, 1.4 μg of pXBPsIG or the molar equivalent of other expression plasmids was used in combination.

ChIP. BCBL-1 cells were transfected using 4 μg of DNA. After 24 h, the cells were harvested and chromatin immunoprecipitation (ChIP) assays performed using a ChIP assay kit (Upstate Biotechnology). Chromatin extracts, cross-linking, sonication, immunoprecipitation, agarose bead elution, and protein removal were carried out according to the manufacturer's instructions. DNA recovered from immunoprecipitates with a His tag-specific polyclonal antibody was used as a template for PCR amplifications. The ORF50, ORF73, and DNAJB6 promoters were amplified using the primers ORF50 ChIP forward (5′-CAA AGA GCT TGG GGG GGC AGA-3′) and ORF50 ChIP reverse (5′-TGC CAC CCA GCT ACT GGT TTC-3′), ORF73 ChIP forward (5′-TCA GCA CGG GGC GTG ATG GCG-3′) and ORF73 ChIP reverse (5′-GCA TTT CAA AGA TAA GGG TG-3′), and DNAJB6 ChIP forward (5′-AAT AAG AGC CCG GAT GCT GAA G-3′) and DNAJB6 ChIP reverse (5′ GCT TCT TGG ATC CAG TGT TTT GG-3′), respectively.

Lentiviral vector transduction. PEL cells (8×10^5) or 5×10^4 HEK293T r219-9 cells were transduced with lentiviral vectors at an input equivalent to a multiplicity of infection of 5 on HEK 293-T cells. At 48 h posttransduction, the cells were analyzed by flow cytometry. The transduced cells were fixed, permeabilized, and stained for RTA expression by using a monoclonal antibody to KSHV RTA in parallel with 12-*O*-tetradecanoyl-phorbol 13-acetate (TPA)-treated and untreated controls. KSHV RTA was visualized using an allophycocyanin-conjugated anti-mouse IgG secondary antibody, allowing EmGFP expression and RTA expression to be monitored simultaneously without requiring compensation.

Confocal microscopy. HEK 293T r219-9 cells were generated by spinoculating HEK 293T cells with tissue culture supernatant from butyrate-treated Vero cells harboring recombinant KSHV.219 (rKSHV.219). Spinoculation was performed at $500 \times g$ for 60 min. These cells were either not treated or transduced with a multiplicity of infection of 5 of G-P (shRNA-GFP expressing) or X-P (shRNA-XBP expressing) lentiviral vectors. At 48 h posttransduction, these cells were seeded at an equal density and treated overnight with 4 mM DTT. Cells were washed and cultured normally for 36 h prior to imaging by laser scanning confocal microscopy (Zeiss Axiovert 100 TV) using Lasersharp 2000 (Bio-Rad).

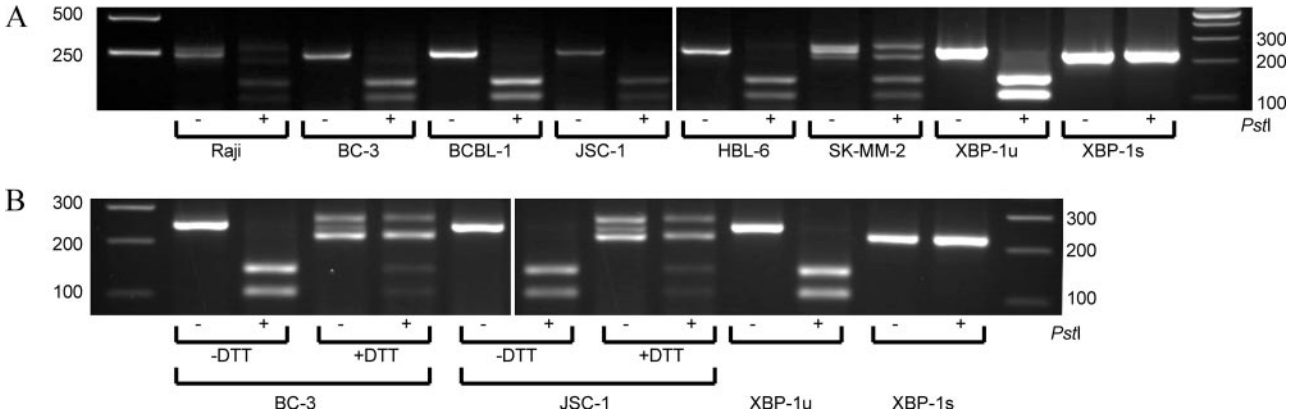

FIG. 1. XBP-1 is unspliced in PEL, but splicing is induced by ER stress. (A) RT-PCR amplification across the XBP-1 intron produces a 249-base-pair amplicon from XBP-1u mRNA and a 223-base-pair amplicon from XBP-1s mRNA. PstI digests only the XBP-1u amplicon. RT-PCR amplification from the Burkitt's lymphoma cell line Raji, the PEL cell lines BC-3, BCBL-1, JSC-1, and HBL-6, and the multiple myeloma cell line SK-MM-2 mRNA shows that XBP-1s is produced in SK-MM-2 cells. In these cells, a slower-migrating, non-PstI-digestible PCR hybrid between XBP-1s and XBP-1u products is visible, similar to hybrids described previously (37). (B) RT-PCR amplification from BC-3 or JSC-1 cells mRNA cultured normally or treated for 1 h with 2 mM DTT. XBP-1s and XBP-1u controls were amplified from pXBPsIG and pXBPuIG, respectively. Composite images of the same gel are shown.

Cells were excited at 488 nm to image enhanced GFP (EGFP) fluorescence and singly excited at 568 nm to image DsRed expression with negligible EGFP excitation.

Recombinant KSHV production. HEK 293-T clone 6 cells (1×10^7; 293T BAC36-6) harboring KSHV BAC36 under hygromycin selection were transfected with 2.8 μg of pXBPsIG and molar equivalents of pIG, pXBPuIG, or pCMV-RTA. All mixes were made up to 2.8 μg with pBluescript II KS+. At 72 h posttransfection, filtered tissue culture supernatants were used to spinoculate 1×10^5 HEK 293-T cells in the presence of 15 μg/ml polybrene. Infected EGFP-positive cells were quantified at 48 h postinfection by flow cytometry.

cDNA labeling and hybridization for microarrays. Total RNA was prepared as described above. The quantity and quality of RNA were evaluated using an Agilent 2100 bioanalyzer (Agilent, West Lothian, United Kingdom). Total RNA (25 μg) was primed using anchored oligo(dT) and a pool of KSHV gene-specific 3′ primers (0.2 μmol) and reverse transcribed into Cy5-dCTP labeled cDNA by using a CyScribe first-strand cDNA labeling kit (GE Healthcare) according to the manufacturer's protocol. Following cDNA labeling, residual RNA was denatured, and unincorporated nucleotides were removed by filtering them through Microcon YM-30 columns (Millipore). Cy5-labeled cDNA was mixed 1:1 with Cy3-labeled cDNA synthesized from a custom-made reference RNA (batched mixture of TPA-induced JSC-1 and HeLa total RNA).

The array elements for the KSHV genes were described previously (19). In addition, 934 array probes to the host genes were PCR amplified from the IMAGE lymphochip clone set (MRC Gene service). Both the host and KSHV array probes were spotted onto aminosalane-coated slides (Schott, Stafford, United Kingdom) in quadruplicates, using a QArray^2 microarrayer (Genetix, New Milton, United Kingdom). The array slides were postprocessed and hybridized with a Cy5/Cy3 mixture under coverslips in an array hybridization chamber (Ambion) at 65°C for 20 h. Microarrays were washed, dried, and scanned using a GenePix 4000B scanner (Axon Instruments).

Data were analyzed as described previously (20) with modifications. Briefly, data were extracted from microarray image files by using GENEPIX PRO 4.0 software (Axon Instruments). The signal-to-noise ratios for individual spots were calculated by dividing the spot signal by the local background. The $\log_2$ median of ratios (Cy5/Cy3) was filtered to remove all flagged data and spots with signal-to-noise ratios of <2 in both the Cy3 and Cy5 channels. The median expression ratio from the quadruplicate spots of each array probe was used for subsequent analysis. The expression ratios generated from each array were assembled and filtered for genes present in all the arrays. The filtered data were median centered for both genes and arrays in Cluster (12) to normalize both the host and viral genes. The normalized data of the viral genes were removed from the matrix, which was then readjusted by median centering in Cluster to order and compare the host genes only. Data were grouped by average linkage hierarchical clustering, using the uncentered Pearson correlation coefficient as the similarity metric. The ordering of the nodes produced by clustering data from 15 arrays was first determined with Cluster by using a one-dimensional self-organizing map, with the number of nodes set to *n*. The clustered data were visualized using TREEVIEW (12). For the KSHV cluster, the normalized data of only the viral genes were grouped by average linkage hierarchical clustering, using the uncentered Pearson correlation coefficient as the similarity metric.

Microarray data accession number. The microarray data are publicly available under Gene Expression Omnibus accession number GSE9096.

RESULTS

XBP-1 is unspliced in PEL cell lines, but splicing is induced by ER stress. We have previously shown that PEL cells have the gene expression profile of plasmablasts (20). The UPR is weakly upregulated in PEL cells (20, 39), and ATF6 is expressed and processed to a 50-kDa transcriptionally active form indicative of a UPR (20). Although the plasma cell transcription factor XBP-1 is expressed in PEL cells, whether XBP-1 mRNA is processed by IRE1 to the highly active transcription factor isoform XBP-1s is unknown. We therefore investigated the splice status of XBP-1 mRNA in different PEL cell lines.

The human XBP-1 mRNA contains a PstI restriction enzyme site within the 26-nucleotide intron excised by IRE1. Based upon an assay described previously (5), we used oligonucleotide primers flanking this region and PstI digestion to distinguish between XBP-1u and XBP-1s RT-PCR products. The PEL cell lines BC-3, BCBL-1, JSC-1, and HBL-6 all express XBP-1u, whereas the plasma cell leukemia cell line SK-MM-2 clearly contained both XBP-1u and XBP-1s, consistent with its more differentiated phenotype (Fig. 1A). This indicates that XBP-1 mRNA is not processed by IRE1 in PEL cells, despite the presence of processed ATF6, indicative of a UPR.

The lack of XBP-1 mRNA processing in PEL cell lines suggests either that the UPR is defective in these cells or that despite ATF6 processing, there is insufficient ER stress to activate IRE1. To distinguish between these two possibilities, we investigated the ability of IRE1 to process XBP-1 mRNA in PEL cells following the chemical induction of ER stress. DTT is a reducing agent that inhibits disulfide bond formation, resulting in the accumulation of misfolded proteins in the ER

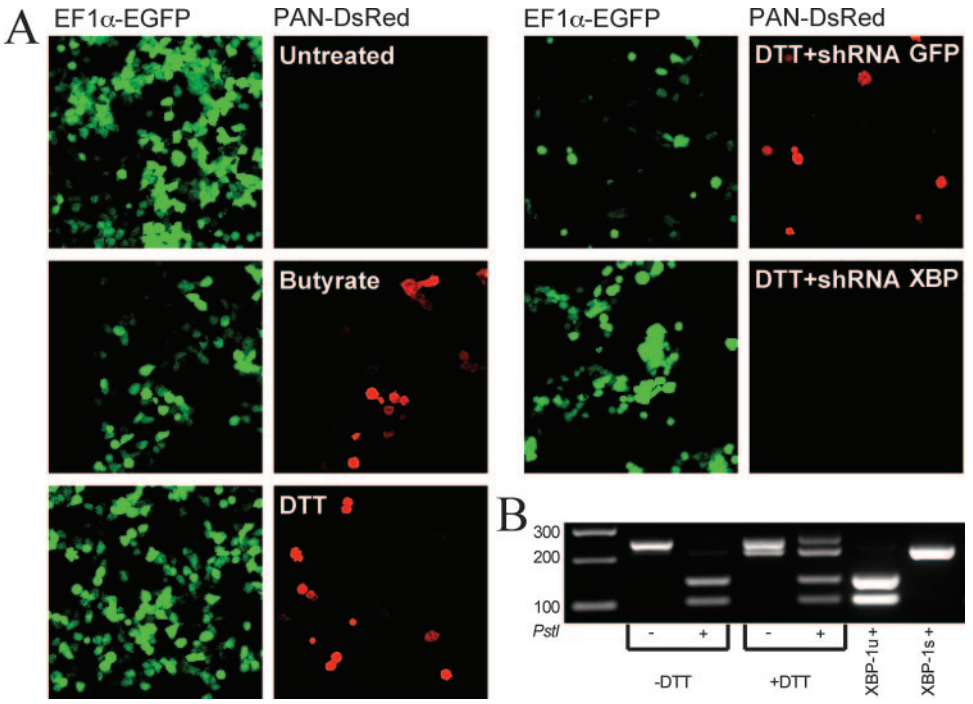

FIG. 2. ER stress induces KSHV lytic replication in an XBP-1-dependent manner. (A) 293T cells harboring recombinant KSHV rKSHV.219 (293T r219-9 cells) were stimulated to induce the KSHV lytic cycle by sodium butyrate or 4 mM DTT treatment overnight. At 48 h posttreatment, cells were analyzed using confocal microscopy. Typical fields singly excited with 488-nm light to detect cells expressing EGFP from the EF1α promoter (green) or 568 nm light to detect cells expressing DsRed from the KSHV lytic cycle PAN promoter (red) are shown magnified at ×60. 293T r219-9 cells were also transduced with lentiviral vectors expressing shRNA XBP-1 or shRNA GFP and treated with DTT as described above. (B) RT-PCR amplification for detection of XBP-1 splicing from 293T r219-9 cell mRNA untreated or treated with DTT.

and induction of the UPR. A 1-hour DTT treatment of the PEL cell lines JSC-1 and BC-3 resulted in efficient XBP-1s processing (Fig. 1B), demonstrating that the machinery responsible for detecting ER stress and processing XBP-1 mRNA is functional in PEL cells.

Endogenous XBP-1s expression results in KSHV reactivation from latency. The observation that DTT induced XBP-1s production led us to consider whether endogenous IRE1 activity results in induction of KSHV lytic replication through XBP-1s. We therefore generated an HEK 293T cell line harboring latent recombinant rKSHV.219, which encodes EGFP driven by the human EF-1α promoter and DsRed driven by the KSHV PAN promoter (41). All infected cells express EGFP, and KSHV lytic replication is marked by DsRed expression. Following DTT treatment, KSHV enters the lytic cycle in a substantial proportion of cells (~15%) (Fig. 2A), consistent with the induction of XBP-1s processing (Fig. 2B). This reactivation is prevented by an shRNA specific for XBP-1 but not by an shRNA specific for the EGFP transcript (Fig. 2A). This shows that endogenous activation of XBP-1s expression can cause KSHV reactivation from latency.

Overexpression of XBP-1 in PEL cells activates RTA expression. The lack of XBP-1 mRNA processing in PEL cell lines and the ability of DTT to induce processing and KSHV lytic replication led us to consider the effect of overexpressing XBP-1s in PEL cells. To efficiently deliver unspliced XBP-1u and spliced XBP-1s in PEL cells, we used the lentiviral vectors XBPuIG (expressing XBP-1u), XBPsIG (expressing XBP-1s), and IG (empty vector), whose vector genomes (Fig. 3A) are encoded by the plasmids pXBPuIG, pXBPsIG, and pIG, respectively. These vectors also express internal ribosome entry site-driven EmGFP from the same transcript as XBP-1, enabling identification of transduced cells and providing a surrogate marker of XBP-1 expression. XBP-1 protein was expressed at levels detectable by Western blotting in the transduced PEL cells (data not shown). The effect of XBP-1u and XBP-1s expression on KSHV was monitored by immunofluorescence and flow cytometry for KSHV regulator of transcription activation (RTA) expression, using a monoclonal antibody to RTA (29). KSHV ORF50 encodes the viral RTA whose expression is necessary and sufficient for initiation of the full KSHV lytic replication program (25). Induction of RTA expression was limited to transduced, EmGFP-expressing cells. All PEL cell lines tested, including the EBV-negative PEL cell lines BCP-1 and BC-3 (data not shown), expressed significant RTA following XBP-1s expression (Fig. 3B). These data indicate that overexpression of XBP-1 in PEL cells induces KSHV RTA expression. Overexpressed XBP-1u is a weak inducer of RTA expression, whereas overexpressed XBP-1s is a potent inducer of RTA expression in the context of latently infected PEL cells.

XBP-1s expression in PEL cells changes the pattern of B-cell gene expression. XBP-1s expression in PEL cell lines is also likely to affect the patterns of B-cell gene expression and the phenotype of the B cell. XBP-1s-transduced PEL cells become larger and uniformly round by light microscopy (data

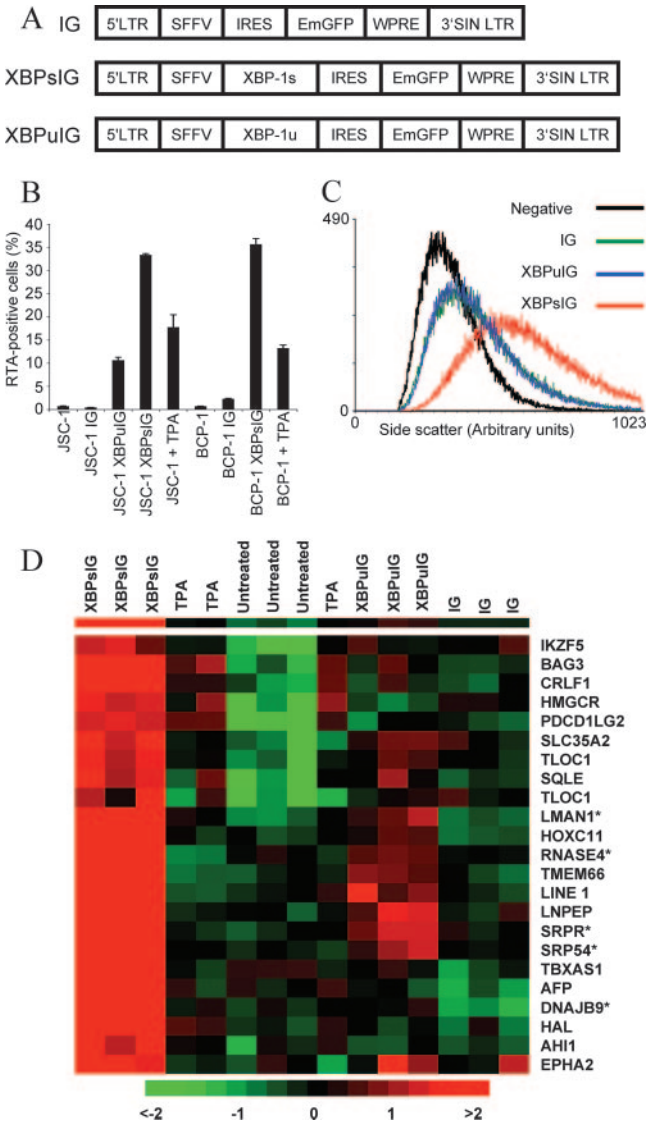

FIG. 3. XBP-1 expression in PEL cells induces KSHV lytic replication and expands the secretory apparatus mimicking plasma cell differentiation. (A) Schematic representation of the lentiviral vector genomes used for the expression of XBP-1s and XBP-1u. LTR, long terminal repeat; SFFV, spleen focus-forming virus long terminal repeat promoter; IRES, internal ribosome entry site; WPRE, woodchuck hepatitis virus posttranscriptional regulatory element; 3′SIN LTR, 3′ self-inactivating long terminal repeat. (B) Percentages of RTA-positive PEL cells at 48 h posttransduction with the vectors described above or following TPA treatment. Error bars represent standard errors for triplicate experiments. Percentages were generated by two-parameter flow cytometric analysis. (C) Side scatter histograms generated by flow cytometry of JSC-1 cells at 48 h posttransduction with the vectors described above. (D) Hierarchical clustering of the normalized expression ratios of a subset of host genes. Labeled cDNA from JSC-1 cells that were untreated, TPA treated (TPA), or transduced with the lentiviral vectors described for panel A was hybridized to microarrays in triplicate. Each column represents one condition and each row one gene. Gene expression is shown as a pseudocolored representation of $\log_2$ expression ratios with red being above and green below the row/column median level of expression (set to 0), as shown by the scale. Asterisks denote genes which are expressed more highly in plasma cells than in B cells (35).

not shown), consistent with the increase in side scatter of over 65% as measured by flow cytometry for the XBP-1s PEL cells (Fig. 3C). This was similar to the previously described phenotype of XBP-1s overexpression in the B-cell line Raji. There, the increase in side scatter was attributed to an expansion of the B-cell secretory apparatus (35). To explore the effect of XBP-1s on PEL gene expression, we determined the enrichment of upregulated genes in XBP-1s-transduced PEL cells compared to that in untransduced and TPA-induced PEL, thereby controlling for the effect of KSHV lytic gene expression (Fig. 3D). Of the subset of genes induced by XBP-1s, five, DNAJB9, SRP54, RNASE4, SRPR, and LMAN1, were previously shown to be induced in Raji cells by XBP-1s (35). Together, these data suggest that XBP-1s expression in PEL cells is able to drive the cells toward a phenotype that is reminiscent of plasma cells.

RTA induction by XBP-1s is sufficient to initiate the full KSHV lytic cycle. We investigated whether the induction of RTA by XBP-1s is sufficient to initiate a full productive lytic cycle. Using a gene expression microarray to monitor the expression of all KSHV genes (19) makes it clear that XBP-1s induces the full lytic cascade in transduced JSC-1 PEL cells (Fig. 4A). Staining XBP-1-transduced PEL cell pellets shows that the KSHV early lytic antigen KbZIP is expressed in XBP-1s-transduced cells to a high level (Fig. 4B). To investigate whether XBP-1s could induce infectious particle production, we used HEK 293T cells stably harboring recombinant KSHV BAC36, which expresses EGFP (45). These cells were transfected with the plasmid expression clones for XBP-1u (pXBPuIG), His-tagged XBP-1s (pXBPsIG), or a control empty vector (pIG), and tissue culture supernatants were subsequently harvested and used to infect HEK 293T cells. Infected cells were quantified by flow cytometry. Importantly, infectious KSHV is produced following expression of XBP-1s, but not XBP-1u, in HEK 293T cells (Fig. 4C). Together, these data show that XBP-1s is an effective inducer of the full KSHV lytic cycle.

XBP-1s transactivates the KSHV ORF50 promoter, synergizes with RTA, and specifically associates with the promoter in PEL cells. KSHV ORF50 encodes KSHV RTA; we therefore investigated the ability of XBP-1 to activate the ORF50 promoter by use of a luciferase reporter gene downstream of a deletion series of the ORF50 promoter, using transient-transfection assays (Fig. 5A). HEK 293T cells were transfected with the XBP-1 expression plasmids pXBPuIG and pXBPsIG or a control empty vector (pIG) in combination with the luciferase reporter gene constructs. Overexpression of XBP-1u resulted in a modest (twofold) activation of the full-length ORF50 promoter, whereas overexpression of XBP-1s resulted in greater activation of the ORF50 promoter. By use of promoter deletions, the XBP-1s response element was mapped to the 200 base pairs preceding the RTA start codon (Fig. 5B and E). As XBP-1s can transactivate the ORF50 promoter in HEK 293T cells, we investigated whether XBP-1s interacts with the ORF50 promoter in PEL cells. We utilized the C-terminal His-tagged XBP-1s expressed from pXBPsIG to perform ChIP assays using the PEL cell line BCBL-1. BCBL-1 cells were transfected with empty vector pIG or pXBPsIG, and XBP-1s was immunoprecipitated using an anti-His monoclonal antibody from cross-linked protein-DNA complexes. The ORF50

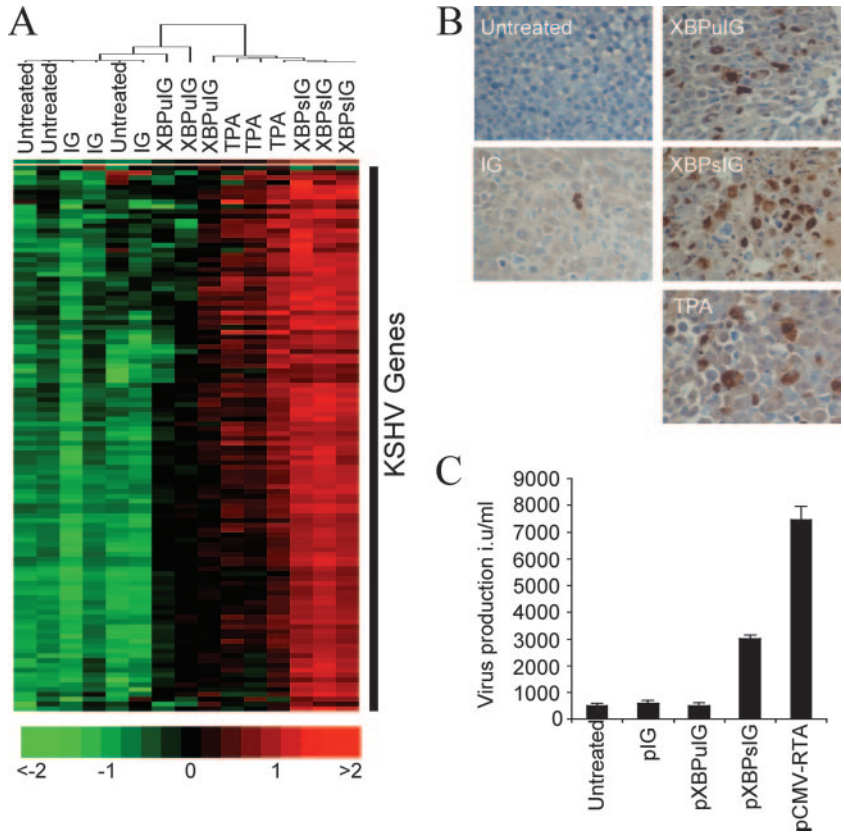

FIG. 4. XBP-1s expression results in reactivation and recombinant KSHV production. (A) Hierarchical clustering of the normalized expression ratios for the KSHV genes (113 probes) from the microarrays as described in the legend to Fig. 3. (B) Cell clots of JSC-1 cells transduced with lentiviral vectors as described in the legend to Fig. 3A were fixed, paraffin embedded, and stained for lytic KbZIP expression visualized using DAB (brown) counterstained with hematoxylin (blue). (C) HEK 293T BAC36-6 cells (1×10^7; harboring KSHV BAC36) were transfected with the plasmid pXBPsIG and molar equivalents of pIG, pXBPuIG, or pCMV-RTA. At 72 h posttransfection, virus release was quantified by infecting HEK 293Ts and monitoring infection after 48 h by flow cytometry. KSHV infectious units (i.u) are defined as the number of green fluorescent cells (KSHV BAC36 infected) per 2×10^5 cells infected with 1 ml of virus-containing supernatant.

promoter was easily detectable in the immune precipitate by PCR (Fig. 5C). XBP-1s does not associate with the KSHV ORF73 latency promoter but does associate with the known XBP-1s responsive promoter of DNAJB9. These data indicate that XBP-1s associates specifically with the authentic ORF50 promoter in BCBL-1 cells, explaining its transactivation activity.

Using a similar ORF50 promoter/DsRed-express reporter assay, we investigated the potential role of an XBP-1 binding site at nucleotides 71826 to 71840 (NC 003409) in the ORF50 intron and the abilities of XBP-1s and RTA to cooperate in activating the ORF50 promoter. The full-length and deletion series of the DsRed/ORF50 promoter behave in the same way as the luciferase assays (Fig. 5D and E). Importantly, the presence of the ORF50 intron did not rescue the promoter activities of the promoter deletions past the ATG-proximal 200 base pairs of the promoter, indicating that the XBP-1s responsive element is within 200 base pairs of the RTA start codon. Using the DsRed reporter assay, the synergy between RTA and XBP-1s was investigated. RTA and XBP-1s resulted in a six- and fourfold increases in DsRed expression, respectively, whereas XBP-1u had no effect (Fig. 5F). When cotransfected with RTA, XBP-1u resulted in an eightfold increase in DsRed expression compared with the control level. Interestingly, XBP-1s synergized with RTA, producing a 15-fold increase in DsRed expression. Together, these data suggest that XBP-1s is sufficient to directly activate the ORF50 promoter and can synergize with RTA.

DISCUSSION

Here, we show that the plasma cell transcription factor XBP-1s is sufficient to initiate a productive KSHV lytic cycle and alter the phenotype of PEL cells. XBP-1s initiates the KSHV lytic cycle by transactivating the KSHV immediate-early gene ORF50. We propose therefore that plasma cell differentiation, and the appearance of XBP-1s, is a cue for KSHV reactivation from latency in B cells. XBP-1 could be detected in association with the ORF50 promoter by using ChIP and synergized with RTA on the ORF50 promoter. The precise mechanism of XBP-1s induction of the KSHV lytic cycle is not known. XBP-1s may bind as a homodimer to an XBP-1s response element in the ORF50 promoter. Alternatively, XBP-1s could bind as a heterodimer by partnering different bZIP proteins. One potential binding partner is the UPR transcription factor ATF6, which is processed to an ac-

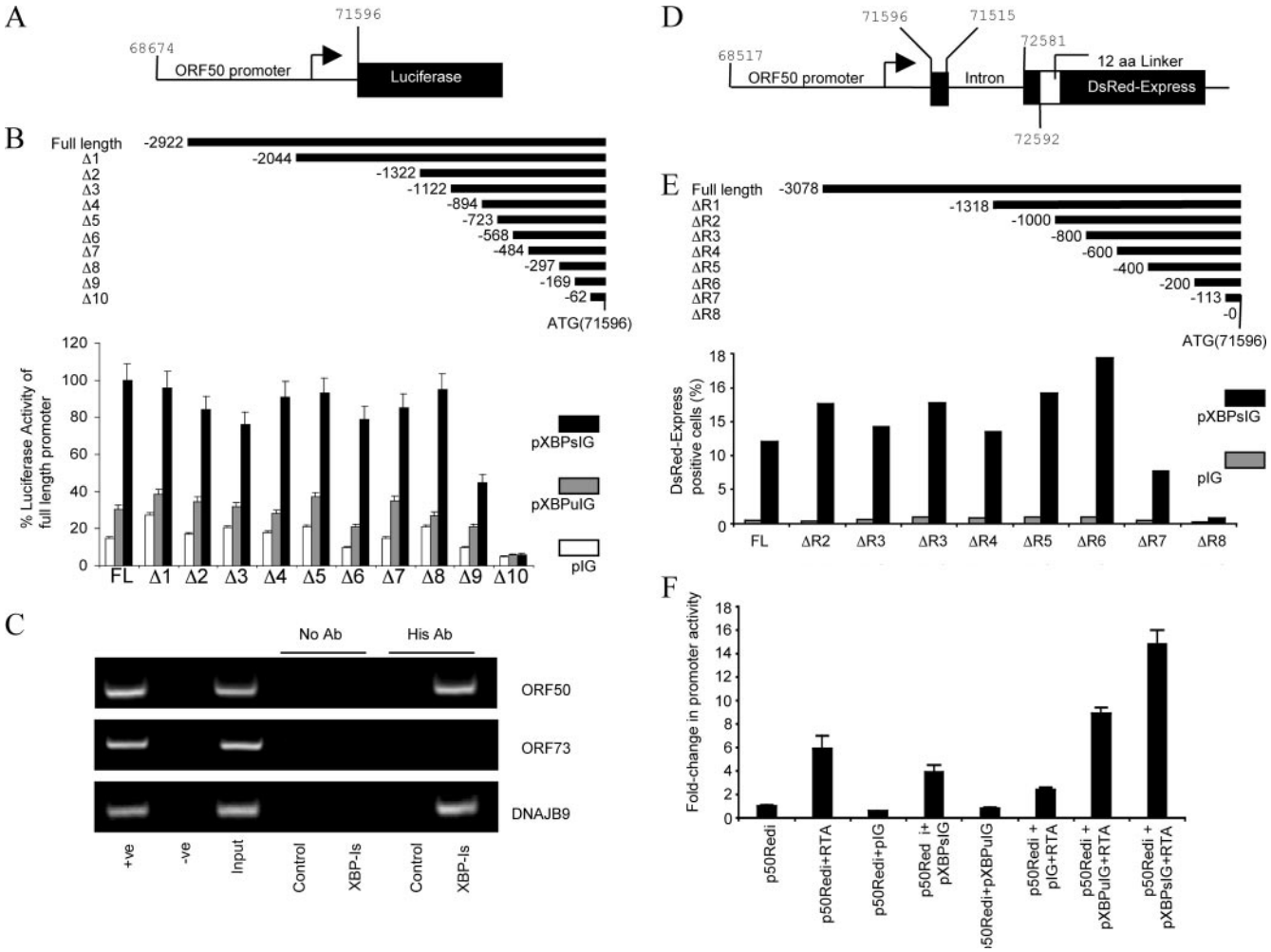

FIG. 5. XBP-1s specifically associates with the KSHV ORF50 promoter, activates ORF50 expression, and synergizes with KSHV RTA in this activity. (A) A schematic representation of the ORF50 promoter used to construct the deletion series of the luciferase reporter constructs. Nucleotide numbers are relative to the KSHV genome sequence NC 003409. (B) HEK 293T cells were transfected with a luciferase reporter plasmid in addition to either pIG (control), pXBPuIG (XBP-1u), or pXBPIG (XBP-1s). At 48 h posttransfection, cells were harvested and luciferase activity was recorded and plotted as a percentage of the activity of the full-length promoter. (C) Chromatin precipitation of XBP-1s. BCBL-1 cells were transfected with pIG or pXBPsIG (which encodes His-tagged XBP-1s). At 48 h posttransfection, cell lysates were immunoprecipitated and PCR amplifications of the KSHV ORF50 promoter, ORF73 promoter, and human DNAJB9 promoter from input, no-antibody controls (No Ab), or immunoprecipitates with anti-HIS (His Ab) were performed. (D) A schematic representation of the ORF50 promoter, including the ORF50 intron, used to construct the deletion series of the DsRed reporter constructs. (E) HEK 293T cells were transfected with a DsRed reporter plasmid in addition to pXBPuIG (XBP-1u) or pXBPIG (XBP-1s), and the percentage of DsRed-express-positive cells was quantified at 48 h posttransfection by flow cytometry. (F) HEK 293T cells were transfected with the full-length ORF50 promoter DsRed reporter plasmid (p50Redi) and pXBPsIG or the molar equivalents of pIG, pXBPuIG, or pCMV-RTA. Half the amount of pXBPsIG, pXBPuIG, pIG, or pCMV-RTA was used in dual transcription factor transfections. The percentages of DsRed-express-positive cells were quantified as described for panel C and are plotted as changes (*n*-fold) in promoter activity.

tive form in PEL cells and known to heterodimerize with XBP-1 (28).

Many potential inducers of the KSHV lytic cycle have been proposed (42). However, few are considered in the context of inducing lytic reactivation in an anatomical site that would favor transmission. XBP-1s fulfills such criteria by potentially allowing KSHV lytic reactivation from latently infected B cells as they terminally differentiate into plasma cells at mucosal surfaces. The lymphoid tissue of the nasopharynx that comprises the Waldeyers ring is infected by KSHV (7, 11), and the virus is able to lytically infect oral epithelial cells (21) and is detectable in saliva samples of infected individuals. Together, this suggests that KSHV is present as a latent infection in an as-yet-undefined B-cell compartment in the oral mucosa, is triggered into lytic replication as the B cells differentiate, and is shed into saliva.

A similar mechanism is proposed for EBV (40), with EBV able to enter lytic replication in plasma cells (23) and epithelial cells (30) and transmit horizontally via saliva. Recently, murine XBP-1s was identified as a factor inducing EBV lytic replication. However, it induced the EBV lytic cycle only in the context of activated protein kinase D, and direct association with either the RTA or ZTA EBV lytic promoters could not be demonstrated, suggesting that murine XBP-1s only indirectly

induces the EBV lytic cycle (4). Of note, human XBP-1 was recently identified in a screen for cellular genes that induce KSHV lytic replication in latently infected KS-1 cells (44). Although not further characterized by Yu et al. (43), the cDNA identified encodes XBP-1u (GenBank accession number BC012841.1), accounting for its low activity level on the ORF50 promoter, data which parallel our findings in PEL cells. Subsequently, murine XBP-1s but not XBP-1u was shown to activate the ORF50 promoter in PEL cells (43), supporting our findings but highlighting potential differences between murine and human XBP-1u.

It is intriguing that KSHV uses a master regulator of the UPR as a lytic switch. Many viruses induce ER stress as a consequence of virus replication and viral glycoprotein maturation. It is now becoming clear that viruses interact closely with the ER stress pathways, possibly inducing functions helpful to the virus (i.e., increased protein folding), while blocking detrimental functions (i.e., translational arrest and apoptosis) (for a review, see reference 42). However, only three viral proteins, hepatitis C virus envelope E1/E2, herpes simplex virus $\gamma_1$34.5, and human cytomegalovirus US11, have been shown to function as ER stress modifiers. The full extent of virus interaction with and manipulation of the ER stress response is not known (16). Our data show that KSHV responds to the UPR directly and therefore may reactivate under many different stress-inducing conditions. However, by reactivating in a cell undergoing a "physiological UPR," the secretory apparatus will be expanded in the absence of translational arrest, providing an ideal environment for the manufacture and release of herpes virions. Whether KSHV specifically modulates components of the UPR during the completion of its lytic replication cycle remains to be determined.

These data further define the partial activation state of the UPR within PEL cells as active ATF6 (20) but inactive XBP-1. Under normal cellular conditions, ATF6 is retained in the ER as a type II membrane protein by the ER unfolded protein sensor GRP78/BiP. Under conditions of ER stress, ATF6 dissociates from GRP78/BiP, translocates to the Golgi apparatus, and is cleaved by Golgi resident proteases S1P and S2P to release the active N-terminal bZIP transcription factor domain. However, in PEL, the signals that result in ATF6 dissociation from Grp78/BiP are clearly different from those that result in IRE1 activation and subsequent XBP-1 processing. Under ER stress conditions, ATF6 and XBP-1 processing usually occur together. Our data show that it is possible for ATF6 to be activated in the absence of XBP-1 activation, possibly through glycosylation status sensing mechanisms (17). IRE1 is functional in PEL when ER stress is induced using DTT (Fig. 1), but it is unclear whether the lack of XBP-1s processing is due to a further defect in PEL or the presence of KSHV or whether it represents an alternative control of the UPR during physiological expansion of the ER in B cells (18, 35).

The active form of XBP-1 has been shown to induce the expression of a range of cellular genes and dramatically alters the phenotype of the B cell in which it is overexpressed (35). XBP-1s expression in PELs also induces a large increase in the granularity of the cells and a decrease in cell proliferation, consistent with previous observation in Raji cells (35). Five genes identified as being XBP-1 responsive in Raji cells overexpressing XBP-1s are also induced in PEL. Together, this suggests that the active XBP-1 expression in B-cell lymphoma cell lines is sufficient to change their phenotypes so that they bear a greater resemblance to that of a plasma cell. It will be interesting to explore the full range of XBP-1 responsive genes in PEL since this type of lymphoma, being plasmablastic, provides the correct cellular transcriptional environment, namely, $BCL6^-$ and $BLIMP\text{-}1^+$, to explore the final stages of plasma cell development.

The proteasome inhibitor and antitumor drug bortezomib (Valcade) inhibits NF-κB activation and induces ER stress, with both mechanisms contributing to tumor cell death. Bortezomib is a potent antimyeloma drug and acts to induce ER stress, inhibit IRE1-mediated XBP-1u processing, and stabilize the XBP-1u protein (24). Bortezomib has recently been shown to have similar antitumor activity on PEL (1). Bortezomib blocked NF-κB activity, inhibited cell proliferation, and induced apoptosis in PEL, but its effects on the UPR were not investigated (1). It is possible that proteasome inhibition induces ER stress and results in KSHV lytic induction through XBP-1u stabilization, thereby contributing to the PEL cell death observed with bortezomib. Recently, bortezomib was shown to be an effective therapy against certain EBV lymphomas (46), raising the possibility that bortezomib could be effective in the treatment of other herpesvirus-associated tumors. With the recognition that the UPR constitutes a plethora of targets for drug development and that the UPR is involved in the replication of many viruses, a new range of antiviral drugs that target UPR pathways may be uncovered.

ACKNOWLEDGMENTS

We gratefully acknowledge K. Ueda for the RTA monoclonal antibody and D. Ganem for the anti-k-bZIP antibody. Two recombinant KSHVs were used, and we are grateful to J. Vieira for rKSHV.219 and S. J. Gao for KSHV BAC36. The lentivirus vector genomes pCSBX/pIG and pEMW were kind gifts from Y. Ikeda, and the lentiviral packaging clones p8.91 and pMDG were kind gifts from D. Trono. We thank R. Jenner for his thoughtful comments on the manuscript and R. Weiss for his support.

S.J.W. and L.D.-G. are supported by the MRC, E.H.T. by a grant from Cancer Research UK, A.W. by grants from the Wellcome Trust and Yorkshire Cancer Research, and P.K. by grants from the Wellcome Trust and Cancer Research UK.

REFERENCES

1. **An, J., Y. Sun, M. Fisher, and M. B. Rettig.** 2004. Antitumor effects of bortezomib (PS-341) on primary effusion lymphomas. Leukemia **18:**1699–1704.
2. **Bertolotti, A., Y. Zhang, L. M. Hendershot, H. P. Harding, and D. Ron.** 2000. Dynamic interaction of BiP and ER stress transducers in the unfolded-protein response. Nat. Cell Biol. **2:**326–332.
3. **Besnier, C., Y. Takeuchi, and G. Towers.** 2002. Restriction of lentivirus in monkeys. Proc. Natl. Acad. Sci. USA **99:**11920–11925.
4. **Bhende, P. M., S. J. Dickerson, X. Sun, W. H. Feng, and S. C. Kenney.** 2007. X-box-binding protein 1 activates lytic Epstein-Barr virus gene expression in combination with protein kinase D. J. Virol. **81:**7363–7370.
5. **Calfon, M., H. Zeng, F. Urano, J. H. Till, S. R. Hubbard, H. P. Harding, S. G. Clark, and D. Ron.** 2002. IRE1 couples endoplasmic reticulum load to secretory capacity by processing the XBP-1 mRNA. Nature **415:**92–96.
6. **Cesarman, E., Y. Chang, P. S. Moore, J. W. Said, and D. M. Knowles.** 1995. Kaposi's sarcoma-associated herpesvirus-like DNA sequences in AIDS-related body-cavity-based lymphomas. N. Engl. J. Med. **332:**1186–1191.
7. **Chagas, C. A., L. H. Endo, E. Sakano, G. A. Pinto, P. Brousset, and J. Vassallo.** 2006. Detection of herpesvirus type 8 (HHV8) in children's tonsils and adenoids by immunohistochemistry and in situ hybridization. Int. J. Pediatr. Otorhinolaryngol. **70:**65–72.
8. **Chang, Y., E. Cesarman, M. S. Pessin, F. Lee, J. Culpepper, D. M. Knowles, and P. S. Moore.** 1994. Identification of herpesvirus-like DNA sequences in AIDS-associated Kaposi's sarcoma. Science **266:**1865–1869.

9. **Clements, M. O., A. Godfrey, J. Crossley, S. J. Wilson, Y. Takeuchi, and C. Boshoff.** 2006. Lentiviral manipulation of gene expression in human adult and embryonic stem cells. Tissue Eng. **12:**1741–1751.
10. **Dupin, N., T. L. Diss, P. Kellam, M. Tulliez, M. Q. Du, D. Sicard, R. A. Weiss, P. G. Isaacson, and C. Boshoff.** 2000. HHV-8 is associated with a plasmablastic variant of Castleman disease that is linked to HHV-8-positive plasmablastic lymphoma. Blood **95:**1406–1412.
11. **Duus, K. M., V. Lentchitsky, T. Wagenaar, C. Grose, and J. Webster-Cyriaque.** 2004. Wild-type Kaposi's sarcoma-associated herpesvirus isolated from the oropharynx of immune-competent individuals has tropism for cultured oral epithelial cells. J. Virol. **78:**4074–4084.
12. **Eisen, M. B., P. T. Spellman, P. O. Brown, and D. Botstein.** 1998. Cluster analysis and display of genome-wide expression patterns. Proc. Natl. Acad. Sci. USA **95:**14863–14868.
13. **Fais, F., G. Gaidano, D. Capello, A. Gloghini, F. Ghiotto, S. Roncella, A. Carbone, N. Chiorazzi, and M. Ferrarini.** 1999. Immunoglobulin V region gene use and structure suggest antigen selection in AIDS-related primary effusion lymphomas. Leukemia **13:**1093–1099.
14. **Flynn, G. C., J. Pohl, M. T. Flocco, and J. E. Rothman.** 1991. Peptide-binding specificity of the molecular chaperone BiP. Nature **353:**726–730.
15. **Gaidano, G., A. Gloghini, V. Gattei, M. F. Rossi, A. M. Cilia, C. Godeas, M. Degan, T. Perin, V. Canzonieri, D. Aldinucci, G. Saglio, A. Carbone, and A. Pinto.** 1997. Association of Kaposi's sarcoma-associated herpesvirus-positive primary effusion lymphoma with expression of the CD138/syndecan-1 antigen. Blood **90:**4894–4900.
16. **He, B.** 2006. Viruses, endoplasmic reticulum stress, and interferon responses. Cell Death Differ. **13:**393–403.
17. **Hong, M., S. Luo, P. Baumeister, J. M. Huang, R. K. Gogia, M. Li, and A. S. Lee.** 2004. Underglycosylation of ATF6 as a novel sensing mechanism for activation of the unfolded protein response. J. Biol. Chem. **279:**11354–11363.
18. **Iwakoshi, N. N., A. H. Lee, P. Vallabhajosyula, K. L. Otipoby, K. Rajewsky, and L. H. Glimcher.** 2003. Plasma cell differentiation and the unfolded protein response intersect at the transcription factor XBP-1. Nat. Immunol. **4:**321–329.
19. **Jenner, R. G., M. M. Alba, C. Boshoff, and P. Kellam.** 2001. Kaposi's sarcoma-associated herpesvirus latent and lytic gene expression as revealed by DNA arrays. J. Virol. **75:**891–902.
20. **Jenner, R. G., K. Maillard, N. Cattini, R. A. Weiss, C. Boshoff, R. Wooster, and P. Kellam.** 2003. Kaposi's sarcoma-associated herpesvirus-infected primary effusion lymphoma has a plasma cell gene expression profile. Proc. Natl. Acad. Sci. USA **100:**10399–10404.
21. **Johnson, A. S., N. Maronian, and J. Vieira.** 2005. Activation of Kaposi's sarcoma-associated herpesvirus lytic gene expression during epithelial differentiation. J. Virol. **79:**13769–13777.
22. **Klein, U., A. Gloghini, G. Gaidano, A. Chadburn, E. Cesarman, R. Dalla-Favera, and A. Carbone.** 2003. Gene expression profile analysis of AIDS-related primary effusion lymphoma (PEL) suggests a plasmablastic derivation and identifies PEL-specific transcripts. Blood **101:**4115–4121.
23. **Laichalk, L. L., and D. A. Thorley-Lawson.** 2005. Terminal differentiation into plasma cells initiates the replicative cycle of Epstein-Barr virus in vivo. J. Virol. **79:**1296–1307.
24. **Lee, A.-H., N. N. Iwakoshi, K. C. Anderson, and L. H. Glimcher.** 2003. Proteasome inhibitors disrupt the unfolded protein response in myeloma cells. Proc. Natl. Acad. Sci. USA **100:**9946–9951.
25. **Lukac, D. M., R. Renne, J. R. Kirshner, and D. Ganem.** 1998. Reactivation of Kaposi's sarcoma-associated herpesvirus infection from latency by expression of the ORF 50 transactivator, a homolog of the EBV R protein. Virology **252:**304–312.
26. **Matolcsy, A., R. G. Nador, E. Cesarman, and D. M. Knowles.** 1998. Immunoglobulin VH gene mutational analysis suggests that primary effusion lymphomas derive from different stages of B cell maturation. Am. J. Pathol. **153:**1609–1614.
27. **Nador, R. G., E. Cesarman, A. Chadburn, D. B. Dawson, M. Q. Ansari, J. Sald, and D. M. Knowles.** 1996. Primary effusion lymphoma: a distinct clinicopathologic entity associated with the Kaposi's sarcoma-associated herpes virus. Blood **88:**645–656.
28. **Newman, J. R., and A. E. Keating.** 2003. Comprehensive identification of human bZIP interactions with coiled-coil arrays. Science **300:**2097–2101.
29. **Okuno, T., Y. B. Jiang, K. Ueda, K. Nishimura, T. Tamura, and K. Yamanishi.** 2002. Activation of human herpesvirus 8 open reading frame K5 independent of ORF50 expression. Virus Res. **90:**77–89.
30. **Pegtel, D. M., J. Middeldorp, and D. A. Thorley-Lawson.** 2004. Epstein-Barr virus infection in ex vivo tonsil epithelial cell cultures of asymptomatic carriers. J. Virol. **78:**12613–12624.
31. **Pica, F., and A. Volpi.** 2007. Transmission of human herpesvirus 8: an update. Curr. Opin. Infect. Dis. **20:**152–156.
32. **Polson, A. G., L. Huang, D. M. Lukac, J. D. Blethrow, D. O. Morgan, A. L. Burlingame, and D. Ganem.** 2001. Kaposi's sarcoma-associated herpesvirus K-bZIP protein is phosphorylated by cyclin-dependent kinases. J. Virol. **75:**3175–3184.
33. **Reimold, A. M., N. N. Iwakoshi, J. Manis, P. Vallabhajosyula, E. Szomolanyi-Tsuda, E. M. Gravallese, D. Friend, M. J. Grusby, F. Alt, and L. H. Glimcher.** 2001. Plasma cell differentiation requires the transcription factor XBP-1. Nature **412:**300–307.
34. **Schroder, M., and R. J. Kaufman.** 2005. The mammalian unfolded protein response. Annu. Rev. Biochem. **74:**739–789.
35. **Shaffer, A. L., M. Shapiro-Shelef, N. N. Iwakoshi, A. H. Lee, S. B. Qian, H. Zhao, X. Yu, L. Yang, B. K. Tan, A. Rosenwald, E. M. Hurt, E. Petroulakis, N. Sonenberg, J. W. Yewdell, K. Calame, L. H. Glimcher, and L. M. Staudt.** 2004. XBP1, downstream of Blimp-1, expands the secretory apparatus and other organelles, and increases protein synthesis in plasma cell differentiation. Immunity **21:**81–93.
36. **Shamu, C. E., and P. Walter.** 1996. Oligomerization and phosphorylation of the Ire1p kinase during intracellular signaling from the endoplasmic reticulum to the nucleus. EMBO J. **15:**3028–3039.
37. **Shang, J., and M. A. Lehrman.** 2004. Discordance of UPR signaling by ATF6 and Ire1p-XBP1 with levels of target transcripts. Biochem. Biophys. Res. Commun. **317:**390–396.
38. **Shapiro-Shelef, M., and K. Calame.** 2005. Regulation of plasma-cell development. Nat. Rev. Immunol. **5:**230–242.
39. **Swift, S., A. Tucker, V. Vinciotti, N. Martin, C. Orengo, X. Liu, and P. Kellam.** 2004. Consensus clustering and functional interpretation of gene-expression data. Genome Biol. **5:**R94.
40. **Thorley-Lawson, D. A., and A. Gross.** 2004. Persistence of the Epstein-Barr virus and the origins of associated lymphomas. N. Engl. J. Med. **350:**1328–1337.
41. **Vieira, J., and P. M. O'Hearn.** 2004. Use of the red fluorescent protein as a marker of Kaposi's sarcoma-associated herpesvirus lytic gene expression. Virology **325:**225–240.
42. **West, J. T., and C. Wood.** 2003. The role of Kaposi's sarcoma-associated herpesvirus/human herpesvirus-8 regulator of transcription activation (RTA) in control of gene expression. Oncogene **22:**5150–5163.
43. **Yu, F., J. Feng, J. N. Harada, S. K. Chanda, S. C. Kenney, and R. Sun.** 2007. B cell terminal differentiation factor XBP-1 induces reactivation of Kaposi's sarcoma-associated herpesvirus. FEBS Lett. **581:**3485–3488.
44. **Yu, F., J. N. Harada, H. J. Brown, H. Deng, M. J. Song, T. T. Wu, J. Kato-Stankiewicz, C. G. Nelson, J. Vieira, F. Tamanoi, S. K. Chanda, and R. Sun.** 2007. Systematic identification of cellular signals reactivating Kaposi sarcoma-associated herpesvirus. PLoS Pathog. **3:**e44.
45. **Zhou, F. C., Y. J. Zhang, J. H. Deng, X. P. Wang, H. Y. Pan, E. Hettler, and S. J. Gao.** 2002. Efficient infection by a recombinant Kaposi's sarcoma-associated herpesvirus cloned in a bacterial artificial chromosome: application for genetic analysis. J. Virol. **76:**6185–6196.
46. **Zou, P., J. Kawada, L. Pesnicak, and J. I. Cohen.** 2007. Bortezomib induces apoptosis of Epstein-Barr virus (EBV)-transformed B cells and prolongs survival of mice inoculated with EBV-transformed B cells. J. Virol. **81:**10029–10036.